Journal of Ethnopharmacology 337 (2025) 118915

Contents lists available at ScienceDirect

Journal of Ethnopharmacology

journal homepage: www.elsevier.com/locate/jethpharm

Mexican calea (*Calea zacatechichi* Schltdl.) interferes with cholinergic and dopaminergic pathways and causes neuroglial toxicity

Maria Rita Garcia [a,b,c,d,e], Federico Ferreres [f], Tiago Mineiro [d,e], Romeu A. Videira [a], Ángel Gil-Izquierdo [g], Paula B. Andrade [a], Vítor Seabra [d,e], Diana Dias-da-Silva [b,c,d,e,h], Nelson G.M. Gomes [a,*]

[a] *REQUIMTE/LAQV, Laboratório de Farmacognosia, Departamento de Química, Faculdade de Farmácia, Universidade do Porto, R. Jorge Viterbo Ferreira, n° 228, 4050-313, Porto, Portugal*
[b] *Associate Laboratory i4HB - Institute for Health and Bioeconomy, Faculty of Pharmacy, University of Porto, Rua Jorge de Viterbo Ferreira 228, Porto, 4050-313, Portugal*
[c] *UCIBIO, Laboratory of Toxicology, Faculty of Pharmacy, University of Porto, R. Jorge Viterbo Ferreira, n° 228, 4050-313, Porto, Portugal*
[d] *Associate Laboratory i4HB - Institute for Health and Bioeconomy, University Institute of Health Sciences - CESPU, 4585-116, Gandra, Portugal*
[e] *UCIBIO - Applied Molecular Biosciences Unit, Forensics and Biomedical Sciences Research Laboratory, University Institute of Health Sciences (1H-TOXRUN, IUCS-CESPU), 4585-116, Gandra, Portugal*
[f] *Molecular Recognition and Encapsulation (REM) Group, Department of Food Technology and Nutrition, Universidad Católica de Murcia, 30107, Murcia, Spain*
[g] *Research Group on Quality, Safety and Bioactivity of Plant Foods, Department of Food Science and Technology, CEBAS (CSIC), Campus University Espinardo, 30100, Murcia, Spain*
[h] *LAQV/REQUIMTE, ESS, Polytechnic of Porto, Rua Dr. António Bernardino de Almeida, 4200-072, Porto, Portugal*

ARTICLE INFO

Handling Editor: V Kuete

Keywords:
Chlorogenic acid
Entheogen
Nictoflorin
Oneiromancy
Psychoactive
Rutin

ABSTRACT

Ethnopharmacological relevance: The use of "*Mexican calea*" (*Calea zacatechichi* Schltdl.) in ritualistic ceremonies, due to its dream-inducing effects, was until recently limited to indigenous communities in Mexico. However, the plant has recently gained popularity in Western societies being commonly used in recreational settings. Despite the traditional and recreational uses, mechanisms underlying its reported oneirogenic effects remain unknown, with no data available on its neurotoxic profile.

Aim of the study: The scarcity of toxicological data and the unknown role of major neurotransmitter systems in the dream-inducing properties of the plant prompted us to investigate which neurotransmitters might be affected upon its consumption, as well as the potential cytotoxic effects on neurons and microglial cells. Furthermore, we aimed to explore a relationship between the recorded effects and specific constituents.

Materials and methods: Effects on cholinergic and monoaminergic pathways were investigated using enzymatic assays, with the latter also being conducted in neuronal SH-SY5Y cells along with the impact on glutamate-induced excitotoxicity. Investigation of the neurotoxic profile was approached in neuronal SH-SY5Y and microglial BV-2 cells, evaluating effects on metabolic performance and membrane integrity using MTT and LDH leakage assays, respectively. Potential interference with oxidative stress was monitored by assessing free radical's levels, as well as 5-lipoxygenase mediated lipid peroxidation. Phenolic constituents were identified through HPLC-DAD-ESI(Ion Trap)MS^n analysis.

Results: Based on the significant inhibition upon acetylcholinesterase ($p < 0.05$) and tyrosinase ($IC_{50} = 60.87 \pm 7.3$ μg/mL; $p < 0.05$), the aqueous extract obtained from the aerial parts of *C. zacatechichi* interferes with the cholinergic and dopaminergic systems, but has no impact against monoamine oxidase A. Additionally, a notable cytotoxic effect was observed in SH-SY5Y and BV-2 cells at concentrations as low as 125 and 500 μg/mL ($p < 0.05$), respectively, LDH leakage suggesting apoptosis may occur at these concentrations, with necroptosis observed at higher ones. Despite the neurocytotoxic profile, these effects appear to be independent of radical stress, as the *C. zacatechichi* extract scavenged nitric oxide and superoxide radicals at concentrations as low as 62.5 μg/mL, significantly inhibiting also 5-lipoxygenase ($IC_{50} = 72.60 \pm 7.3$ μg/mL; $p < 0.05$). Qualitative and

* Corresponding author.
E-mail addresses: ritagarcia7@hotmail.com (M.R. Garcia), fferreres@ucam.edu (F. Ferreres), tmarquesmineiro@hotmail.com (T. Mineiro), rvideira@ff.up.pt (R.A. Videira), angelgil@cebas.csic.es (Á. Gil-Izquierdo), pandrade@ff.up.pt (P.B. Andrade), vitor.seabra@iucs.cespu.pt (V. Seabra), dds@ess.ipp.pt (D. Dias-da-Silva), ngomes@ff.up.pt (N.G.M. Gomes).

https://doi.org/10.1016/j.jep.2024.118915
Received 12 July 2024; Received in revised form 4 October 2024; Accepted 5 October 2024
Available online 9 October 2024
0378-8741/© 2024 The Authors. Published by Elsevier B.V. This is an open access article under the CC BY license (http://creativecommons.org/licenses/by/4.0/).

quantitative analysis using HPLC-DAD-ESI(Ion Trap)MS^n enabled the identification of 28 constituents, with 24 of them being previously unreported in this species. These include a series of dicaffeoylquinic, caffeoylpentoside, and feruloylquinic acids, along with 8 flavonols not previously known to occur in the species, mainly 3-*O*-monoglycosylated derivatives of quercetin, kaempferol, and isorhamnetin.

Conclusions: Our findings regarding the neuroglial toxicity elicited by *C. zacatechichi* emphasize the necessity for a thorough elucidation of the plant's toxicity profile. Additionally, evidence is provided that the aerial parts of the plant inhibit both acetylcholinesterase and tyrosinase, potentially linking its psychopharmacological effects to the cholinergic and dopaminergic systems, with an apparent contribution from specific phenolic constituents previously unknown to occur in the species. Collectively, our results lay the groundwork for a regulatory framework on the consumption of *C. zacatechichi* in recreational settings and contribute to elucidating previous contradictory findings regarding the mechanisms underlying the dream-inducing effects of the plant.

1. Introduction

Endemic to Central America and southeastern Mexico, the plant *Calea zacatechichi* Schltdl., commonly known as '*Mexican calea*' and '*dream herb*', is traditionally used among indigenous communities in ritualistic ceremonies but also in medicinal practices (Díaz, 1979; Josabad Alonso-Castro et al., 2012; Mata et al., 2022). Particularly among the Chontal Indians of Oaxaca, *C. zacatechichi* is also used for divination purposes, claimed to enable the obtaining of divine messages during sleep concerning diseases, lost objects, and the future (Mata et al., 2022; Mayagoitia et al., 1986). Usually consumed either by infusion or through inhalation, by smoking or by putting the leaves under the pillow, *C. zacatechichi* leads to psychoactive effects that translate into somnolence, a relaxing feeling of well-being, intensified visual imagery, and vivid/lucid dreaming (Mata et al., 2022; Mayagoitia et al., 1986). Additionally, ethnomedicinal surveys indicate that the leaves are used for their analgesic, antipyretic, antidiabetic, antidiarrheal and antiemetic effects, but mainly as a herbal treatment for various inflammatory conditions (Josabad Alonso-Castro et al., 2012; Leonti et al., 2003; Venegas-Flores et al., 2002).

Even though therapeutic properties have been allegedly associated with the plant, in 2013, the United Nations Office on Drugs and Crime (UNODC) included this oneirogenic plant in their list of plants of concern (United Nations Office on Drugs and Crime, 2013). *C. zacatechichi* is among a pool of new psychoactive substances (NPS) that have been increasingly flooding the European and US markets and online vendors, many of which being labelled as legal despite causing effects similar to those of illegal narcotics (European Monitoring Centre for Drugs and Drug Addiction, 2022). In addition to the empirical and common perception among consumers that herbal highs are safe (Graziano et al., 2016), there are few reports covering the toxicity profile of *C. zacatechichi*, and even fewer supporting its dream-inducing (i.e., oneirogenic) effects. Moreover, throughout the literature, *C. zacatechichi* and *Calea ternifolia* Kunth are often erroneously employed as taxonomic synonyms, along with a wide list of synonyms and the disagreement in recognizing subordinated taxa in the species, that further blurs the analysis of the plant (Mata et al., 2022).

Such scientific conjecture, characterized by the scarcity of data on the chemical, pharmacological, and toxicological profile of the plant, also contributes to legal inconsistencies regarding its possession and use. For example, Poland remains the only country in Europe restricting its use, while in the US it is classified as illegal only in Louisiana state (González-Yáñez et al., 2019; Mossoba et al., 2016).

First reports on the chemical profile of *C. zacatechichi* evidenced that the plant is particularly rich in sesquiterpene lactones, mainly in germacranolides (Herz and Kumar, 1980; Martinez et al., 1987; Quijano et al., 1979; Wu et al., 2011). Preliminary studies indicate also the occurrence of a series of phenolic constituents, mainly caffeoylquinic acids but also flavonoids, the latter identified as minor constituents (Martinez-Mota et al., 2021; Sałaga et al., 2016). Concerning the mechanisms underlying the oneirogenic effects, available data are poorly characterized. Seminal studies by Díaz and colleagues in human volunteers corroborated data from ethnomedicinal surveys describing increased superficial stages of sleep and heightened visual dream activity (Díaz, 1979; Mayagoitia et al., 1986). Later studies vary in their conclusions, and while the most recent study by Martinez-Mota et al. (2021) suggests the involvement of the noradrenergic system in the increase in Slow Wave Sleep episodes and enhanced fast frequencies of hippocampus during REM sleep in animal models, Wlaź and collaborators solely reported antinociceptive effects with no interference on basic neurological functions (Sałaga et al., 2016).

In short, the mechanisms underlying the dream-inducing properties of *C. zacatechichi* are only minimally understood. We hypothesize that these effects might involve alterations in the monoaminergic and cholinergic systems. Additionally, due to the unclear toxicity profile of the plant, we conducted cell-based experiments using neuronal SH-SY5Y and BV-2 microglial cells to investigate potential neurotoxic effects. Since none of the compounds previously identified in the plant seem to account for these dream-inducing effects, we performed a detailed chemical characterization using HPLC–DAD–ESI(Ion Trap)/MS^n analysis.

2. Material and methods

2.1. General chemicals, reagents and equipment

Isopropanol EMSURE®, methanol (MeOH) LiChrosolv®, perchloric acid and trypan blue were purchased from Merck KGaA (Darmstadt, Germany), ethanol was from Fisher Scientific UK (Loughborough, UK), formic acid from VWR (Fontenay-sous-Bois, France), and dimethylsulphoxide (DMSO) ATRASOL® was from Carlo Erba Reagents (Val de Reuil, France). Remaining solvents and reagents were acquired from Sigma-Aldrich (St. Louis, MO, US), unless stated otherwise.

Cell cultures were maintained in a water-jacketed CO_2 incubator (Toreuse model 2428; St. Louis, MO, US). Samples were freeze-dried on a Virtis SP Scientific Sentry 2.0, Gardiner apparatus (NY, US). Spectrophotometric measurements were performed using a Multiskan™ GO microplate reader (Thermo Fisher Scientific Oy, Vantaa, Finland) and fluorescence determinations were carried out using a BioTek Cytation™ 3 microplate reader (Winooski, US).

2.2. Plant material and extraction

Samples of *C. zacatechichi* aerial parts were obtained from an online vendor (batch number 2019212 A P), and a voucher specimen (ME_04) was deposited at LAQV/REQUIMTE, University of Porto. The samples were ground into a fine powder with a mean particle size of $<$910 μm, aqueous extracts being prepared by decoction, mimicking the conventional procedure used by consumers (approximately 5 g of powdered plant material boiled in 500 mL of distilled water for 30 min). Resulting extracts were then filtered through a Whatman® Grade 1 filtration paper, freeze-dried, and properly stored at – 80 °C until analysis.

2.3. Chemical characterization

2.3.1. HPLC–DAD–ESI(Ion Trap)/MS^n qualitative analyses

Analyses were conducted using an Agilent HPLC 1200 series, which included a binary pump (model G1376A), an autosampler (model G1377A) refrigerated at 4 °C (model G1330B), and a degasser (model G1379B). The system was equipped with a diode array detector (DAD) (model G1315D) and a Bruker ion trap HCT Ultra spectrometer with an electrospray ionization interface mass detector in series (Agilent Technologies, Waldbronn, Germany). ChemStation Software (Agilent, v. B.01.03-SR2) and LCMSD software (Agilent, v. 6.1) were used to control the HPLC system and the mass detector, respectively.

Separation was performed on a Kinetex column (5 μm, C18, 100 Å, 150 × 4.6 mm; Phenomenex, Macclesfield, UK), following the chromatographic conditions described by Ferreres et al. (2015) with slight modifications. The mobile phase was delivered at a flow rate of 800 μL/min and consisted of 1% formic acid (A) and methanol (B), starting with 5% B and using a gradient to obtain 60% B at 25 min and 90% B at 30 min. UV spectral data were obtained at 320 and 350 nm (for Fig. 1, an intermediate wavelength of 335 nm was used).

Concerning the MS-based structure elucidation, the ionization conditions were adjusted at 350 °C and 4.0 kV for capillary temperature and voltage, respectively. The nebulizer pressure and flow rate of nitrogen were 65.0 psi and 11 L/min, respectively. Helium was used as the collision gas, with voltage ramping cycles from 0.3 up to 2 V. Mass spectrometry data were acquired in the negative ionization mode. MS^2 and MS^3 were carried out in the automatic mode, on the most abundant fragment ion in MS and MS^2, respectively. The injection volume was of 20 μL and the full scan mass covered the range from *m/z* 100 up to 1500.

2.3.2. HPLC-DAD quantitative analysis

Quantitative analysis was done on an analytical Gilson Medical Electronics HPLC unit (Villiers le Bel, France) coupled with an Agilent 1100 series diode array detector (Agilent Technologies, Waldbronn, Germany), chromatographic data being processed on Clarity software system 8.1.0.77 (DataApex Ltd., Prague, Czech Republic). Separation was performed on a Kinetex column (5 μm, C18, 100 Å, 150 × 4.6 mm; Phenomenex, Macclesfield, UK), under the same conditions as described in the qualitative analysis. Detection wavelengths of 320 nm (for cinnamoyl derivatives) and 350 nm (for flavonoid derivatives) were selected for quantitation.

The phytochemical standards 3-*O*-caffeoylquinic acid (3-CQA), 5-*O*-caffeoylquinic acid (5-CQA), kaempferol-3-*O*-rutinoside, quercetin-3-*O*-rutinoside, quercetin-3-*O*-(6-acetylglucoside), isorhamnetin and isorhamnetin-3-*O*-rutinoside were acquired from Extrasynthese (Genay, France). 3,4-di-*O*-Caffeoylquinic acid (3,4-diCQA), 3,5-di-*O*-caffeoylquinic acid (3,5-diCQA) and 4,5-di-*O*-caffeoylquinic acid (4,5-diCQA) were obtained from Chengdu Biopurify Phytochemicals Ltd. (Sichuan, China). 4-*O*-Caffeoylquinic acid (4-CQA) was from ChemFaces (Wuhan, China) while caffeic acid and quercetin were acquired to Sigma-Aldrich (St. Louis, MO, US).

Calibration curves were built using five different concentration levels of reference standards. Table 1 depicts the information regarding linearity, limits of detection (LOD), and limits of quantification (LOQ). Both LOD and LOQ were calculated from the residual standard deviation (σ) and slope (S) of the regression curves, according to the equations LOD = 3.3σ/S and LOD = 10σ/S.

3-CQA (**1**), 4-CQA (**2**), 5-CQA (**3**), caffeic acid (**5**), 3,4-diCQA (**15**), 3,5-diCQA (**16**), quercetin-3-*O*-rutinoside (**17**), 4,5-diCQA (**20**), kaempferol-3-*O*-rutinoside (**21**), isorhamnetin-3-*O*-rutinoside (**22**), quercetin (**24**), and isorhamnetin (**28**) were quantitated against their own standard curves. Remaining constituents were quantitated against the calibration curves of the structurally most similar compounds i.e., compounds **4**, **13**, **14** and **23** were quantitated as 4-CQA; compounds **6**, **11** and **12** as 5-CQA; compounds **7**–**10** as caffeic acid; compound **18** as

Table 1
Results of linear regression equation analysis, LOD[a] and LOQ[b].

Standards[c]	Regression equation	R^2	LOD (μg/mL)	LOQ (μg/mL)
3-CQA	y = 26.175x - 17.783	0.9957	0.81	2.45
4-CQA	y = 35.486x - 43.236	0.9988	0.18	0.54
5-CQA	y = 35.315x - 173.02	0.9921	1.52	4.62
CA	y = 81.287x + 121.12	0.9994	0.55	1.68
3,4-diCQA	y = 166.84x + 513.44	0.9976	1.08	3.27
3,5-diCQA	y = 109.38x - 332.46	0.9868	0.35	1.06
Qct-3-rut	y = 39.534x + 42.386	0.9995	0.95	2.88
Qct-3-*O*-(6-acetylglucoside)	y = 50.058x + 186.67	0.9905	0.23	0.69
4,5-diCQA	y = 91.139x - 857.76	0.9979	0.94	2.86
Kaempferol-3-rut	y = 32.48x - 26.898	0.9995	0.84	2.54
Isorhamnetin-3-rut	y = 43.747x + 94.915	0.9992	1.21	3.68
Quercetin	y = 61.321x + 71.166	0.9936	0.16	0.48
Isorhamnetin	y = 24.68x + 24.466	0.9975	0.35	1.05

[a] Limit of detection.
[b] Limit of quantification.
[c] CQA: Caffeoylquinic acid; CA: Caffeic acid; diCQA: di-*O*-Caffeoylquinic acid; Qct: Quercetin; rut: Rutinoside.

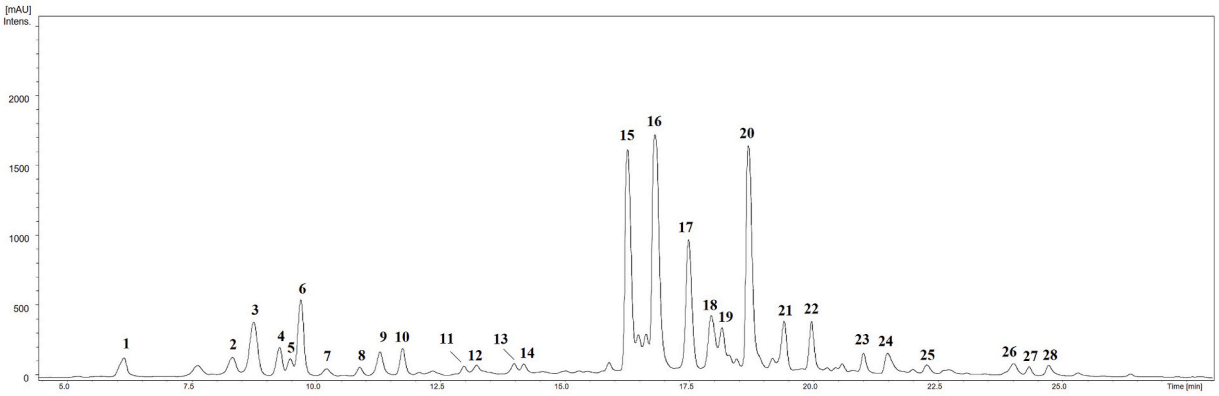

Fig. 1. UV Chromatogram (355 nm) of the aqueous extract obtained from the aerial parts of *C. zacatechichi*. Identity of compounds **1**–**28** as in Table 2.

3,5-diCQA; compound **19** as quercetin-3-*O*-(6-acetylglucoside); compound **25** as isorhamnetin-3-*O*-rutinoside; compound **26** as kaempferol-3-*O*-rutinoside; compound **27** as quercetin-3-*O*-rutinoside.

2.4. Cellular assays

2.4.1. Cell culture

Human neuroblastoma SH-SY5Y and mouse microglia BV-2 cells were purchased from ATCC® (Manassas, Virginia, US). SH-SY5Y cells were maintained in DMEM + GlutaMAX™:F12 culture medium, while BV-2 cells were maintained in DMEM + GlutaMAX™, both supplemented with 10% heat-inactivated foetal bovine serum (FBS) and 1% PenStrep solution (penicillin 5000 U/mL and streptomycin 5000 μg/mL). Cells were cultured at 37 °C in a humidified atmosphere containing 5% CO_2. Culture media, FBS and PenStrep were obtained from GIBCO, Invitrogen (Grand Island, NY, US).

For evaluation of impact on cell viability, cells were seeded in 96-well plates at a density of 40 000 cells/well, while for the inhibition of monoamine oxidase A (MAO-A) activity cells were seeded in T25 flasks at a density of 30 000 cells/cm^2 and exposed to each treatment for 24 h.

2.4.2. MTT reduction assay

The impact on cellular viability was assessed in both SH-SY5Y and BV-2 cells by evaluating mitochondrial activity through the 3-(4,5-dimethylthiazol-2-yl)-2,5-diphenyltetrazolium (MTT) reduction assay (Ribeiro et al., 2021). Briefly, after seeding 24 h, cells were exposed to the extract, and following a 24 h exposure, the cell culture medium was removed and 100 μL of 10% MTT solution was added to each well and incubated for 90 min. Subsequently, the solution was aspirated, and 200 μL of a mixture of DMSO and isopropanol (3:1) was added to each well to dissolve the formazan crystals. Spectrophotometric results were obtained at 560 nm, results being expressed as a percentage of viability. Triton-X at 1% was used as a positive control.

2.4.3. Membrane integrity assay

Membrane integrity was evaluated using a kinetic NADH oxidation assay with pyruvate as a substrate (Ribeiro et al., 2021). Cells were exposed to the extract for 24 h, 20 μL aliquot of cell culture medium being collected after exposure and mixed with 25 μL of 15 mM pyruvate and 230 μL of 250 μM β-nicotinamide adenine dinucleotide (NADH). Spectrophotometric readings were obtained at 340 nm, results being expressed as the fold increase in absorbance compared to untreated cells. Triton X-100 1% was used as a positive control.

2.4.4. Glutamate-stimuli response

Cellular viability in the presence of glutamate as a toxic stimulus was assessed using SH-SY5Y cells, as previously described (Bernardo et al., 2022). After seeding and incubating the cells for 24 h, a pre-incubation of 3 h with increasing concentrations of the extract was performed, followed by co-incubation with 20 μL of glutamate (300 mM) for the remaining 21 h. Afterwards, the MTT reduction assay was employed as previously described (2.4.2. MTT reduction assay), results being expressed as percentage of viability. Statistical comparisons performed against the positive control.

To evaluate the effect of the mixture (*i.e.*, extract + glutamate), experimental results were compared with simulation results obtained using the Bliss independence principle according to the following equation:

$$\text{Simulation results} = \text{Effect}_{\text{Extract}} + \text{Effect}_{\text{Glutamate}} - \text{Effect}_{\text{Extract}} \times \text{Effect}_{\text{Glutamate}}$$

Statistically significant effects were considered synergistic if increased cytotoxicity was observed, while opposing results were attributed to antagonistic effects.

2.4.5. Evaluation of monoamine oxidase A (MAO-A) activity in neuronal cells

Impact on MAO-A activity was assessed in SH-SY5Y cells according to the protocol described by Andrade and colleagues, with some modifications (Bernardo et al., 2018). Briefly, after exposing the cells to the extract (62.5 μg/mL) and washing them with phosphate-buffered saline (PBS) solution, they were detached and centrifuged (390g, 5 min). Ice-cold PBS (1 mL) was added to the resulting cell pellets and cell lysis was carried out in a Teflon Potter-Elvehjem tissue grinder. Afterwards, an aliquot was used for protein quantification by the Bradford method, while the remaining was used for quantification of MAO-A activity. To attain this, 37.5 μL of kynuramine (100 mM) and phosphate buffer (KH_2PO_4, 0.1M, pH 7.4) were added to 700 μL aliquots of cell suspension, resulting in a final volume of 1 mL. Mixtures were then incubated for 4 h at 37 °C, 100 μL of perchloric acid (0.4M) being added to stop the reaction. Samples were then centrifuged (12 500 g, 10 min), and 500 μL of supernatant was collected from each with an equal volume of NaOH (2N) being added to each sample. The signal intensity was measured using a fluorescence plate reader (excitation at 315 nm; emission at 380 nm). The MAO inhibitor monoamine oxidase inhibitor clorgyline (1 mg/mL) was used as positive control.

2.5. Cell-free enzymatic and antiradical assays

2.5.1. Evaluation of monoamine oxidase A (MAO-A) activity

Impact on the activity of MAO-A (EC 1.4.3.4) was also evaluated in a cell-free system, following the protocol described by Bernardo et al. (2018) with some modifications. Phosphate buffer (KH_2PO_4, 0.1M, pH 7.4), hMAO-A (final concentration 0.015 μg/mL), and extract (final concentration 62.5 μg/mL) were combined to a final volume of 500 μL, with kynuramine (0.75 mM) being added after a 5 min incubation period, and left incubating for additional 15 min at 37 °C. Afterwards, 100 μL NaOH (2N) was added, and the absorbance was read at 314 nm. Clorgyline was used as reference inhibitor.

2.5.2. Evaluation of tyrosinase activity

Impact on the activity of tyrosinase was evaluated according to the modified dopachrome method (Cebollada et al., 2024). In a 96-well plate, 40 μL of extract was mixed with 80 μL of phosphate buffer (0.05 M, pH 6.8), 40 μL of tyrosinase from mushroom (EC 1.14.18.1; 90 U/mL), and 40 μL of L-DOPA (0.85 μM). The kinetic reduction was recorded at 475 nm for 3 min and the results expressed as enzymatic inhibition. Kojic acid was used as reference inhibitor.

2.5.3. Evaluation of acetylcholinesterase activity

Effects upon the activity of acetylcholinesterase (AChE) were approached through the Ellman's method (João et al., 2021). Briefly, 25 μL of extract in Tris-HCl buffer (50 mM, pH = 8) were mixed with 25 μL of acetylcholine iodide (15 mM), 125 μL of 5,5′-dithiobis(2-nitrobenzoic acid) (Ellman's reagent) and 50 μL of 0.1% bovine serum albumin in Tris-HCl buffer (pH = 8). The rates of inhibition were calculated after the addition of 25 μL of AChE Type VI-S (from *Electrophorus electricus*, EC 232-559-3) at 0.44 U/mL (in 0.1% bovine serum albumin in Tris-HCl buffer), absorbance being recorded at 405 nm during 1 min. Galantamine was used as reference inhibitor.

2.5.4. Evaluation of 5-lipoxygenase activity

5-Lipoxygenase (5-LOX) activity was assessed by measuring the oxidation of linoleic acid to conjugated dienes, following the method described in Cebollada et al. (2024). In a 96-well plate, 20 μL of the sample was mixed with 200 μL of $Na_2HPO_4{\cdot}2H_2O$ (0.1 M, pH 9.0) and 20 μL of 5-LOX from soybean (EC 1.13.11.12) at a concentration of 100 U/20 μL. The reaction was initiated by adding 20 μL of linoleic acid (4.18 mM in ethanol), and the formation of its oxidation product was monitored for 3 min at 234 nm. Quercetin was used as inhibitor.

2.5.5. Evaluation of scavenging effects upon nitric oxide and superoxide radicals

The scavenging capacity upon nitric oxide radical ($^{\bullet}NO$) was assessed through the Griess method (Cebollada et al., 2024). To 100 μL of the extracts at various concentrations, 100 μL of sodium nitroprusside (20 mM) was added and incubated for 1 h at room temperature under light exposure. Afterwards, 100 μL of Griess reagent (1% sulphanilamide + 0.1% *N*-(naphth-1-yl)ethylenediamine dihydrochloride, in 2% H_3PO_4) was added and left incubating in the dark for 10 min at room temperature. Absorbances were read at 560 nm and the results were expressed as the percentage of NO levels.

Scavenging effects against superoxide anion radical ($O_2^{\bullet-}$) were also approached through a non-enzymatic model (Cebollada et al., 2024). In a 96 well-plate, 50 μL of extract, 50 μL of NADH 166 μM, 150 μL of nitro blue tetrazolium chloride 43 μM and 50 μL phenazine methosulfate (2.7 μM) were added, and the plates were read at 560 nm for 3 min.

2.6. Statistical analysis

Statistical analysis was performed using GraphPad Prism 8.4.2 Software (San Diego, CA, US). Primarily, the normality of the distribution was determined through the Shapiro-Wilk normality test. Based on the normality, one-way ANOVA followed by Welch's *post hoc* correction was employed to assess the existence of statistically significant differences between treatments and control groups, with p values lower than 0.05 being considered statistically significant. The number of independent experiments and replicates are specified in each figure caption.

3. Results and discussion

3.1. Chemical qualitative and quantitative characterization of C. zacatechichi aerial parts

3.1.1. HPLC–DAD–ESI(Ion Trap)/MS^n qualitative analysis

HPLC–DAD–ESI/MS^n analysis of the aqueous extract obtained from the aerial parts of *C. zacatechichi* has retrieved 28 phenolic compounds. UV and MS data enabled the identification of 19 compounds as cinnamoyl derivates (**1**–**16**, **18**, **20** and **23**) and 9 flavonoid compounds (**17**, **19**, **21**, **22** and **24**–**28**) (Fig. 1, Table 2).

3.1.1.1. Cinnamoyl derivatives. Spectral data (~295sh, 325 nm) of compounds **1**–**16**, **18**, **20** and **23** indicate that they correspond to cinnamoyl derivates (Table 2).

Compound **5** exhibits a deprotonated molecular ion at m/z 179 with loss of a carbonyl (44 amu) fragment resulting in a 135 amu ion indicating the presence of caffeic acid, as corroborated through the comparison with a reference standard.

Molecular ions of constituents **1**–**4** and **6** at m/z 353 indicate that they correspond to caffeoylquinic acids (CQA) (Table 2). Considering the resulting ions and their relative frequency in the MS^2 data, as well as previous results from Clifford et al. (2003), compounds **1**–**3** were identified as 3-CQA (**1**), 4-CQA (**2**) and 5-CQA (**3**), which was corroborated by reference standards. Similar MS fragmentations, as those observed for **2** and **3**, were also shared by compounds **4** and **6**, respectively, indicating that they correspond to isomers and being consequently labelled as (4)-CQA (**4**) and (5)-CQA (**6**) (Table 2).

With a mass of 367, 14 amu higher than CQAs, compounds **11**–**14** correspond to feruloylquinic acids (FQA) (Table 2). Based on their MS fragmentation (Clifford et al., 2003), **11** and **13** were identified as 5-FQA and 4-FQA, respectively, while compounds **12** and **14**, sharing a similar fragmentation, were labelled as (5)-FQA (**12**) and (4)-FQA (**14**).

Compounds **15**, **16**, **18** and **20** display deprotonated molecular ions of 515 amu, 162 amu higher than CQAs, thus indicating that they might correspond to di-caffeoylquinic acids (diCQA), also presenting a base peak at m/z 353 in their MS^2 fragmentations (Table 2). As reported by

Table 2
Rt, UV and MS: [M-H]$^-$, MS^2[M-H]$^-$ and MS^3[(M-H)→base peak]$^-$ data from compounds detected in the aqueous extract of *C. zacatechichi* aerial parts.

Compounds [a]		*R*t (min)	UV (nm)	[M-H]$^-$, m/z	MS^2[M-H]$^-$, m/z (%)	MS^3([M-H]$^-$→base peak), m/z (%)
1	3-CQA	6.1	294sh, 324	353	191(100), 179(30), 135(10)	
2	4-CQA	8.3	295sh, 324	353	191(25), 179(50), 173(100), 135(20)	
3	5-CQA	8.8	294sh, 324	353	191(100)	
4	(4)-CQA	9.3	296sh, 324	353	191(40), 179(70), 173(100), 135(10)	
5	CA	9.5	294sh, 326	179	135(100)	
6	(5)-CQA	9.7	296sh, 326	353	191(100)	
7	CPtA	10.2	296sh, 326	311	179(90), 149(100), 135(10)	
8	CPtA	10.9	298sh, 326	311	179(50), 149(100), 135(15)	
9	CPtA	11.3	296sh, 325	311	179(75), 149(100), 135(10)	
10	CPtA	11.7	298sh, 324	311	179(75), 149(100), 135(20)	
11	5-FQA	13.0	298sh, 322	367	191(100)	
12	(5)-FQA	13.3	296sh, 324	367	191(100), 173(10)	
13	4-FQA	14.0	293sh, 322	367	191(10), 173(100)	
14	(4)-FQA	14.2	298sh, 324	367	191(5), 173 (100)	
15	3,4-diCQA	16.2	298sh, 324	515	353(100), 335(20), 173(50)	191(40), 179 (60), 173 (100)
16	3,5-diCQA	16.9	298sh, 326	515	353(100)	191(100), 179(40)
17	Qct-3-rut	17.5	256, 266sh, 300sh, 350	609	301	
18	(3,5)-diCQA	17.9	294sh, 324	515	353(100)	191(100), 179(70), 173 (60)
19	Qct-3-AcHex	18.2	–	505	463(40), 301(100)	
20	4,5-diCQA	18.7	298sh, 326	515	353(100)	191(40), 179 (40), 173 (100)
21	K-3-rut	19.5	266, 289sh, 346	593	285(100)	
22	Isrh-3-rut	19.9	256, 266sh, 300sh, 352	623	315(100)	
23	3-F-4-CQA	21.0	296sh, 324	529	367(40), 353(100)	191(40), 179 (60), 173 (100)
24	Qct	21.5	256, 266sh, 300sh, 368	301		
25	Isrh-3-rut isomer	22.3	256, 266sh,	623	315(100)	

(*continued on next page*)

Table 2 (*continued*)

Compounds [a]		*Rt* (min)	UV (nm)	[M-H]⁻, *m/z*	MS^2[M-H]⁻, *m/z* (%)	MS^3[M-H]⁻→base peak), *m/z* (%)
			300sh, 348			
26	MeK-3-rut	24.0	266, 354	607	299(100)	
27	diMeQct-3-rut	24.4	256, 266sh, 300sh, 354	637	329(100)	
28	Isrh	24.7	256, 266sh, 300sh, 366	315		

[a] CA: Caffeic acid; F: Ferulic acid; Q: Quinic acid; CQA: Caffeoylquinic acid; FQA: Feruloylquinic acid; CPtA: Caffeoylpentoside acid; Qct: Quercetin; Isrh: Isorhamnetin; K: Kaempferol; Me: Methyl; Ac: Acetyl; Hex: Hexoside; rut: Rutinoside.

Clifford et al. (2003), both 3,4-diCQA and 4,5-diCQA exhibit a MS^3 base peak at *m/z* 173 amu, enabling their distinction by the presence of a secondary ion at 335 amu for 3,4-diCQA, a spectral feature not observed in 4,5-diCQA. Accordingly, compound **15** was identified as 3,4-diCQA, as also confirmed through the comparison with a reference standard, while **20** corresponds to 4,5-diCQA. Showing a MS^3 base peak at 191 amu, characteristic of 3,5-diCQA (Clifford et al., 2003), and confirmed by reference standard, compound **16** was identified as 3,5-diCQA. Due to the resemblance of the MS^2 and MS^3 fragmentation patterns of compound **18** to **16**, the former was labelled as (3,5)-diCQA (**18**).

Compound **23**, with a deprotonated molecular ion at 529 amu, 14 amu higher than that observed for diCQA, indicates the presence of a feruloylcaffeoylquinic acid (FCQA). A base peak at *m/z* 353 alongside a significant ion at 367 were detected in MS^2 spectrum, while in the MS^3 data, in addition to the base peak at *m/z* 173, other abundant ions were verified at 191 and 179 amu (Table 2). Therefore, and according to Clifford et al. (2003), these findings indicate that compound **23** corresponds to 3-feruloyl-4-caffeoylquinic acid.

Compounds **7**–**10** share the same deprotonated molecular ion a 311 amu and MS^2 fragmentation pattern (Table 2) with a 132 amu fragment loss (pentosyl radical), and providing ions at *m/z* 179 ([caffeic ac-H]⁻), a base peak at 149 (caffeoyl radical loss, ([(M-H)-162]⁻) and at 135 ([(M-H)-(132 + 44)]⁻), hence suggesting that they correspond to caffeoylpentoside acid isomers (CPtA).

3.1.1.2. Flavonoids. Presenting characteristic UV spectral data of flavonols, with a free hydroxyl in the 3-position and deprotonated molecular ions at *m/z* 301 and 315 (pentahydroxy-flavone and tetrahydroxy-methoxy-flavone) (Table 2), compounds **24** and **28** were identified as quercetin (3,5,7,3′,4′-pentahydroxy-flavone) and isorhamnetin (3,5,7,4′-tetrahydroxy-3′-methoxy-flavone), respectively.

The UV spectra of compounds **17**, **21**, **22** and **25**–**27** indicate flavonols substituted in the position 3 (Table 2), and while **17**, **22**, **25**, and **27** are disubstituted in the B ring, **21** and **26** are monosubstituted at the 4′-position. In all these compounds, MS^2 fragmentation results reveal the loss of a 308 amu fragment yielding a base peak corresponding to the deprotonated aglycone ion ([aglycone-H]⁻) at *m/z* 301 (**17**), 285 (**21**), 315 (**22** and **25**), 299 (**26**) and 329 (**27**) (Table 2).

The 308 amu fragment indicates a rhamno-hexosyl radical (146 + 162) and the absence of ion between the deprotonated molecular ion and the base peak, corresponding to an interglycosidic linkage, indicates a 1 → 6. As this union is difficultly fragmented, rutinosyl (rhamnosyl(1 → 6)hexoside) is the most frequent disaccharide. Thus, compounds **17** and **21** can be labelled as quercetin-3-*O*-rutinoside (rutin) and kaempferol-3-*O*-rutinoside, respectively. Compounds **22** and **25** are isomers of rutinoside-substituted tetrahydroxy-methoxy-flavones, with isorhamnetin (3,5,7,4′-tetrahydroxy-3′-methoxy-flavone) being the most common; thus, the most abundant isomer **22** can be labelled as isorhamnetin-3-*O*-rutinoside, whereas **25** is the 3-*O*-rutinoside derivative of tamarixetin (3,5,7,3′-tetrahydroxy-4′-methoxy-flavone) or rhamnetin (3,5,3′,4′-tetrahydroxy-7-methoxy-flavone), depending on the glycosidic portion of the compound (rhamnosyl(1 → 6)glucoside/rhamnosyl(1 → 6)galactoside). The deprotonated aglycone of constituent **26** at *m/z* 299 (trihydroxy-methoxy-flavone) (Table 2), likely methylkaempferol, suggests that it can be kaempferide (3,5,7-trihydroxy-4′-methoxy-flavone), thus being labelled as methylkaempferol-3-*O*-rutinoside and tentatively as kaempferide-3-*O*-rutinoside. The deprotonated aglycone of **27** at *m/z* 339 (trihydroxy-dimethoxy-flavone) corresponds to dimethylquercetin (Table 2), hence the compound is labelled as dimethylquercetin-3-*O*-rutinoside.

Compound **19** exhibits a deprotonated molecular ion at *m/z* 505, while the MS^2 fragmentation ion from the aglycone resulted in a base peak *at m/z* 301 (quercetin) that along with the fragment ion at *m/z* 463 (Table 2), resulting from the loss of a 42 amu fragment (acetyl radical), allows to identify it as quercetin-3-*O*-acetylhexoside.

3.1.2. HPLC–DAD quantitative analysis

The quantitative analysis demonstrate that the aqueous extract obtained from *C. zacatechichi* is mainly characterized by the occurrence of hydroxycinnamic acid derivates, constituting *ca.* 61% of the total quantifiable phenolic composition, the remaining corresponding to flavonol derivatives (Table 3). However, the main constituent corresponds to quercetin-3-*O*-rutinoside (**17**) (13.81 ± 0.67 μg/mL), followed by 4,5- and 3,5-di-*O*-caffeoylquinic acids (**20** and **16**) which together constitute 24.15% of the total quantifiable phenolic content (Table 3). Cumulatively, and considering the significant content of kaempferol-3-*O*-rutinoside (**21**; 5.91 ± 0.19 μg/mL), the diglycosylated flavonols **17**

Table 3
Content of phenolic constituents on the aqueous extract obtained from the aerial parts of *C. zacatechichi*.

Peak	Compounds[a]	mg/g (dry extract)[b]	Relative abundance (%)
1	3-CQA	2.37 ± 0.01	2.95
2	4-CQA	3.84 ± 0.17	4.77
3	5-CQA	4.33 ± 0.10	5.38
4	(4)-CQA	1.78 ± 0.08	2.21
5	CA	0.73 ± 0.04	0.91
6	(5)-CQA	4.52 ± 0.42	5.61
7	CPtA	0.16 ± 0.01	0.20
8	CPtA	0.20 ± 0.01	0.25
9	CPtA	0.59 ± 0.01	0.73
10	CPtA	0.59 ± 0.005	0.73
11	5-FQA	0.40 ± 0.02	0.50
12	(5)-FQA	0.39 ± 0.02	0.49
13	4-FQA	0.32 ± 0.01	0.40
14	(4)-FQA	0.28 ± 0.02	0.35
15	3,4-diCQA	4.82 ± 0.38	5.98
16	3,5-diCQA	9.35 ± 0.59	11.60
17	Qct-3-rut	13.81 ± 0.67	17.14
18	(3,5)-diCQA	0.61 ± 0.03	0.76
19	Qct-3-AcHex	0.47 ± 0.02	0.59
20	4,5-diCQA	10.12 ± 0.60	12.55
21	K-3-rut	5.91 ± 0.19	7.34
22	Isrh-3-rut	3.89 ± 0.15	4.83
23	3-F-4-CQA	4.05 ± 0.13	5.03
24	Qct	1.77 ± 0.06	2.20
25	Isrh-3-rut isomer	1.42 ± 0.01	1.76
26	MeK-3-rut	0.93 ± 0.04	1.15
27	diMeQct-3-rut	0.83 ± 0.03	1.03
28	Isrh	2.70 ± 0.01	2.57
	∑	81.18 ± 3.84	100

[a] CA: Caffeic acid; F: Ferulic acid; Q: Quinic acid; CQA: Caffeoylquinic acid; FQA: Feruloylquinic acid; CPtA: Caffeoylpentoside acid; Qct: Quercetin; Isrh: Isorhamnetin; K: Kaempferol; Me: Methyl; Ac: Acetyl; Hex: Hexoside; rut: Rutinoside.

[b] Results expressed as the mean ± standard deviation of three determinations.

and **21** constitute ca. 25% of the total quantifiable phenolic content (Table 3).

Globally, and according to our results, the aqueous extract obtained from the aerial parts of *C. zacatechichi* is mainly characterized by the occurrence of di-*O*-caffeoylquinic acids (*ca.* 30% of the total quantifiable phenolic content) while most flavonols present a 3-O-glycosylation (Table 3).

The early report by Werner Herz described the isolation of acacetin from a $CHCl_3$ extract obtained from aerial parts of *C. zacatechichi* (Herz and Kumar, 1980), being later described also in aqueous extracts (Martinez-Mota et al., 2021; Sałaga et al., 2016). In line with our findings (Tables 2 and 3), Estrada-Reyes also described the hydroxycinnamic acids 3-, 4- and 5-CQA (**1**–**3**), with a similar content, in an aqueous extract obtained from the aerial parts of the plant, but quercetin-3-*O*-rutinoside (**17**) was found to be present in much lower concentration compared to our results (Martinez-Mota et al., 2021). Furthermore, and unlike our results, their UPLC-ESI-MS analysis mostly revealed free flavones, including a significant content of myricetin, combretol and luteolin, which may have resulted from the hydrolysis of their glycosylated counterparts (Martinez-Mota et al., 2021).

It is also worth noting that while we mainly describe the occurrence of caffeoylquinic and feruloylquinic acids (Table 2), Martinez-Mota et al. (2021) suggest the presence of a series of 5-*O*-caffeoylshikimic acid isomers that we could not detect in our extract.

In comparison with previous studies, we identified 24 previously unreported compounds in *C. zacatechichi*. More specifically, a series of hydroxycinnamic acids is here described for the first time, namely the di-*O*-caffeoylquinic acids **15**, **16**, **18** and **20**, several feruloylquinic acid derivatives (**11**–**14**), along with caffeic acid (**5**) and 3-feruloyl-4-caffeoylquinic acid (**23**) (Table 2). In addition to the previously reported quercetin-3-*O*-rutinoside (**17**) (Martinez-Mota et al., 2021), herein described as the main constituent (Table 3), we also report 8 additional flavonols, mainly methylated and glycosylated derivatives of quercetin, kaempferol and isorhamnetin (Table 2).

3.2. *C. zacatechichi induces neuronal cell death with disruption of cytoplasmic membrane in neuronal and microglial cells*

As revealed by the MTT assay, the aqueous extract of *C. zacatechichi* caused a significant interference on the mitochondrial performance of both microglial and neuronal cells (Fig. 2). In BV-2 microglial cells, cytotoxicity was observed only at concentrations higher than 500 μg/mL, resulting in an impairment of metabolic competence down to 13.4% at the highest concentration tested (Fig. 2A). Neuronal SH-SY5Y cells appear to be more susceptible to the effects of *C. zacatechichi*, exhibiting significant decreases at concentrations higher than 125 μg/mL, with reductions in mitochondrial competence exceeding 90% at 500 and 1000 μg/mL (Fig. 2C).

To further detail the neurocytotoxic effects of *C. zacatechichi*, levels of plasma membrane damage was investigated through the lactate dehydrogenase (LDH) assay. As shown in Fig. 2B, disruption of membrane integrity in BV-2 microglial cells, indicated by intracellular content extravasation, is confirmed by a 1.83-fold increase in LDH leakage ($p < 0.01$) upon treatment with 1000 μg/mL. Apoptosis or necroptosis also appears to be the programmed cell death pathways activated in SH-SY5Y neuronal cells when exposed to the extract at concentrations higher than 250 μg/mL, as results showed 2.37-fold ($p < 0.05$), 2.85-fold ($p < 0.001$), and 2.66-fold ($p < 0.01$) increases in LDH leakage (Fig. 2D).

Cumulatively, results from the MTT (Fig. 2A and C) and LDH leakage assays (Fig. 2B and D) indicate that in microglial BV-2 cells at 500 μg/mL, and in neuronal SH-SY5Y cells at 125 μg/mL, apoptosis or other phenomena impairing cell viability, but not necroptosis, may still be occurring. This could explain the decreased mitochondrial competence observed at lower concentrations, although further testing is needed to finely elucidate the cell death mechanisms. In the event that apoptotic cells are not eliminated, they may lose cell membrane integrity and

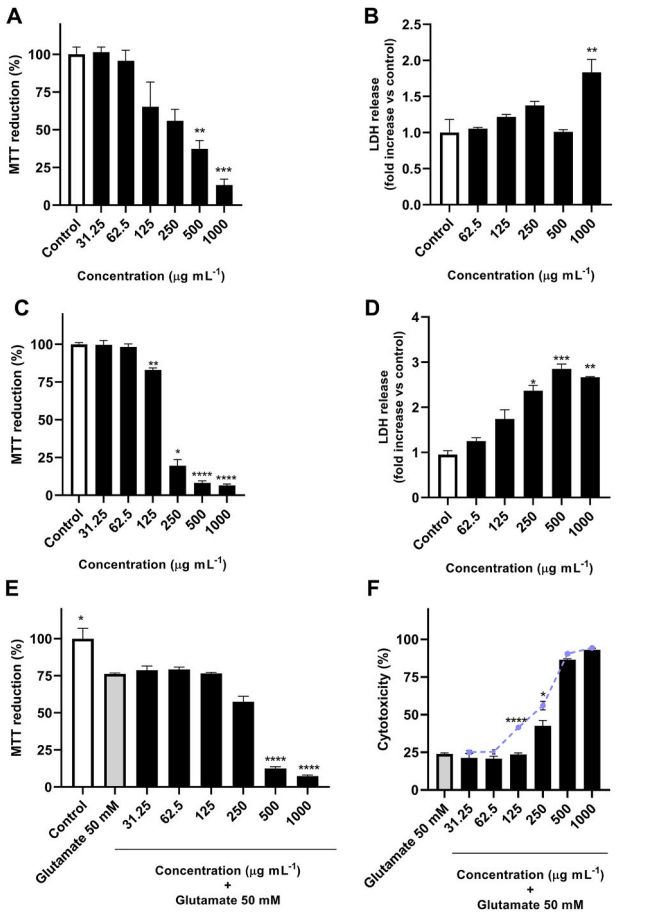

Fig. 2. Effects of *C. zacatechichi* aerial parts extract upon the mitochondrial competence of BV-2 (**A**) and SH-SY5Y (**C**), LDH release in BV-2 (**B**) and SH-SY5Y cells (**D**), and on glutamate-induced excitotoxicity in SH-SY5Y cells (**E**). Assessment of the mixture's effect following glutamate co-incubation (**F**). Results are shown as mean ± SEM from three independent experiments performed in triplicate. Simulated results for addictive effects represented by purple dots. Statistical significance: *$p < 0.05$; **$p < 0.01$; ***$p < 0.001$; ****$p < 0.0001$. (For interpretation of the references to colour in this figure legend, the reader is referred to the Web version of this article.)

release their intracellular contents, which function as damage-associated molecular patterns and can lead to secondary apoptosis (Sachet et al., 2017; Zhao et al., 2021). It is worth noting that the previous study by Mossoba et al. (2016) demonstrated that *C. zacatechichi* can inhibit the transcription factor NF-κB. This inhibition is hypothesized to lead to the accumulation of pro-apoptotic factors such as Bax, Bak, and caspases, and increase vulnerability to inflammatory cytokines, potentially contributing to apoptosis (Verzella et al., 2020). In the central nervous system (CNS), microglial cells are responsible for the efferocytosis process, preventing inflammation and other pathological conditions with the intent of maintaining tissue homeostasis (Zhao et al., 2021) and the observed effects might be explained by their phagocytic activity preventing LDH release.

Indeed, although the LDH release assay is an accurate approach to assess cell viability, one of its limitations is the inability to distinguish LDH release during necroptotic cell death from that occurring in late apoptosis (Kari et al., 2022). To overcome this limitation, complementary assays such as annexin V/propidium iodide staining should be performed in the future to further clarify the underlying cell death pathway triggered by *C. zacatechichi*.

Despite its known dream-inducing effects on the CNS, there have been no prior studies on neurotoxicity associated with the plant. Until now, research on the toxicity profile of *C. zacatechichi* has primarily

focused on assessing cell viability in human erythrocytes, revealing a 73% induction of eryptosis with an aqueous extract at 100 μg/mL (González-Yáñez et al., 2019). Additionally, in proximal tubular kidney HK-2 cells, significant decreases in viability were observed at concentrations starting at 37 μg/mL with a methanol extract (Mossoba et al., 2016).

Impairment of glutamate homeostasis is often cited as a pivotal feature in the neurodegenerative effects induced by various recreational drugs, especially those associated with addiction (Reissner and Kalivas, 2010). Heightened glutamate stimulation exacerbates excitotoxicity, resulting in oxidative damage, elevated Ca^{2+} levels, and mitochondrial dysfunction, culminating in both acute and chronic neurological degeneration (Reissner and Kalivas, 2010). Considering the above, we found it relevant to investigate whether *C. zacatechichi* could worsen glutamate-induced excitotoxicity or instead offer neuroprotection by counteracting the effects of glutamate.

As shown in Fig. 2E and F, glutamate-induced cytotoxicity was exacerbated by *C. zacatechichi* at 500 and 1000 μg/mL, the two highest concentrations of the aqueous extract. Different results were obtained with the extract at 125 and 250 μg/mL as, although these concentrations were cytotoxic *per se*, they neither exacerbated glutamate-induced cytotoxicity as expected nor counteracted its effects, with lower concentrations also remaining cytotoxic (Fig. 2E and F).

3.3. Inhibition of acetylcholinesterase (AChE) and tyrosinase by *C. zacatechichi* contribute to potential changes on the homeostasis of neurotransmitters

Chemical characterization of the aqueous extract obtained from the aerial parts *C. zacatechichi* (Table 3) demonstrated a high content in competent inhibitors of MAO-A, namely in 3,4-diCQA (**15**) and 3,5-diCQA (**16**) that are known to inhibit the enzyme in primary astrocytes and neurons (Lim et al., 2020). Inhibition of MAO-A influences various aspects of neuronal activity, including sleep and dreaming and the increased levels of dopamine, serotonin and norepinephrine, resulting from MAO-A inhibition, are believed to play a role in vivid dreaming (Pagel and Helfter, 2003). This is the case with the MAO-A inhibitor moclobemide, whose adverse effects include nightmares and vivid dreams, and which is also hypothesized to contribute to the psychedelic and dream-inducing effects of Ayahuasca due to its high content of harmala alkaloids (Brito-da-costa et al., 2020). Such rationale prompted us to evaluate the effects of *C. zacatechichi* extract upon MAO-A in neuronal SH-SY5Y cells and in a cell-free assay. Both assays were carried out using 62.5 μg/mL as the highest concentration, as significant cytotoxic effects on SH-SY5Y cells were observed at 125 μg/mL (Fig. 2C). However, no inhibitory effects were detected in either case (data not shown).

Evidence for inducing lucid dreams is even stronger for acetylcholine inhibitors, which increase their frequency by enhancing cholinergic neurotransmission through AChE inhibition (Aru et al., 2020; Gott et al., 2024). The clinical corroboration of the dream-inducing effects of AChE inhibitors is based on the effects of galantamine, results in human volunteers having demonstrated a significant dose-dependent increase in the frequency of lucid dreams, along with enhanced dream recall, vividness, and complexity (LaBerge et al., 2018). Indeed, it is during REM sleep, when acetylcholine levels are high, that most literature suggests dreaming and vivid dreaming occur (Aru et al., 2020).

Oneirogenic plants remain poorly studied, with available information being very limited or nonexistent. However, AchE inhibition appears to be a common mechanism among plants described as having dream-inducing properties or leading to vivid dreaming. This mechanism is observed in several *Huperzia* spp. due to their content of huperzine A (Armijos et al., 2016), as well as in ibogaine, the main alkaloid found in the hallucinogenic and oneirogenic plant *Tabernanthe iboga* (Alper et al., 2012). Furthermore, AchE inhibition has also been suggested as the main mechanism responsible for the oneirogenic effects of *Silene capensis*, with lucid and prophetic dreams being attributed to its triterpenoid saponin content (Oldoni et al., 2024).

While displaying a lower inhibitory capacity than galantamine (IC_{50} = 2.44 ± 0.02 μg/mL), *C. zacatechichi* extract significantly decreased AChE activity in the full range of concentrations, reducing the enzymatic activity by 45.2% at 1000 μg/mL (Fig. 3A), which might partially explain the dream-inducing effects of the plant.

The significant inhibition of AChE by *C. zacatechichi* might be explained by its high content of specific hydroxycinnamic acids, particularly 5-CQA (**3**) and 3,5-diCQA (**16**) (Table 3), both being reported to inhibit the enzyme in vivo (Conforti et al., 2010; Kang et al., 2016). Potential synergistic or cumulative effects with caffeic acid (**5**) are also anticipated, as a significant decrease in AChE activity has been reported both in vitro and in a rat model of Alzheimer's disease (Wang et al., 2016). Structure-activity relationship (SAR) studies indicate that several flavonoids identified in the extract of *C. zacatechichi* meet the structural requirements for enhanced AChE inhibition, specifically the C2-C3 unsaturation in ring C and the polyhydroxylation on rings A and B, that are characteristic features of flavonols (Khan et al., 2018). The main constituent of the extract, i.e., quercetin-3-*O*-rutinoside (**17**), along with the minor constituents quercetin (**24**) and isorhamnetin (**28**), strongly inhibit the enzyme (Khan et al., 2018; Li et al., 2023; Shoukat et al., 2023), and are likely to contribute to the recorded effects (Fig. 3A). However, it should be noted that glycosylation at C3 is reported to decrease the inhibitory capacity upon AChE, and nearly 34% of the quantifiable phenolic constituents correspond to 3-*O*-glycosylated flavonols (Table 3).

While the presence of tyrosinase in the CNS, particularly in the *substantia nigra*, is still a matter of debate, it is well known that besides oxidizing L-DOPA to dopaquinone, tyrosinase may also oxidize dopamine to form melanin pigments under certain circumstances (Jin et al., 2024). The enzyme present in dopaminergic neurons affects dopamine levels and exacerbates its toxicity through conversion into neuromelanin and dopamine quinones (Greggio et al., 2005; Jin et al., 2024), being recently recognized to contribute to the onset of neurodegenerative pathogenesis (Carballo-Carbajal et al., 2019).

As seen in Fig. 3B, treatment with *C. zacatechichi* extract caused a significant reduction in tyrosinase activity across all concentrations, with reductions ranging from 66.3% to 35.0%. However, despite the significant inhibitory effects, the estimated IC_{50} value of 60.87 ± 7.3 μg/mL indicates a lower inhibitory capacity than the reference inhibitor kojic acid (IC_{50} = 1.75 ± 0.03 μg/mL). It is plausible to assume that the high content of quercetin-3-*O*-rutinoside (**17**) on the aqueous extract of *C. zacatechichi* (Table 3) contributes to the strong inhibitory capacity upon tyrosinase, being reported as a competitive inhibitor of the enzyme binding to the active site pocket (Chatatikun et al., 2023; Si et al., 2012). Featuring as the second most abundant flavonoid identified in *C. zacatechichi* extract (Table 3), kaempferol-3-*O*-rutinoside (**21**) displays moderate tyrosinase inhibition with reported IC_{50} values of 59.34 ± 1.5 μg/mL (Viany et al., 2019). While the consensus on the structural requirements of flavonoids for tyrosinase inhibition remains elusive, most flavonoids identified in the *C. zacatechichi* extract conform to the general understanding that hydroxylation at the C5 and C7 positions is an important chemical feature (Jakimiuk et al., 2022; Santi et al., 2019). The potential synergism between the 3-*O*-glycosylated flavonols and hydroxycinnamic acids identified in the extract (Table 2) is also anticipated to contribute to the inhibitory effects on tyrosinase (Fig. 3B). The main phenolic acid identified on the extract, 4,5-diCQA (**20**), is reported as a strong inhibitor of tyrosinase (IC_{50} = 35.36 ± 0.25 μM) (Devkota et al., 2022), while 5-CQA (**3**) chelates a copper cation responsible for sustaining the active state of tyrosinase (Kim et al., 2020).

Based on previous in vivo reports (Díaz, 1979; Martinez-Mota et al., 2021; Mayagoitia et al., 1986; Sałaga et al., 2016), it is clear that *C. zacatechichi* impacts neurotransmission but the only known hypothesis is that it may affect the noradrenergic system due to its in vivo antidepressant-like effects (Martinez-Mota et al., 2021). Herein, we

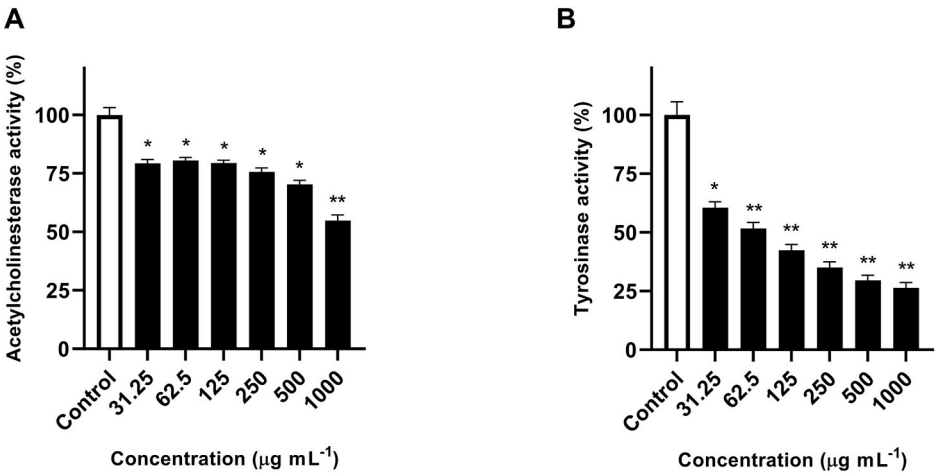

Fig. 3. Effects of *C. zacatechichi* aerial parts extract on the enzymatic activity of acetylcholinesterase (**A**) and tyrosinase (**B**). Results are shown as mean ± SEM from three independent experiments performed in triplicate. Statistical significance: $^{*}p < 0.05$; $^{**}p < 0.01$.

provide further insights on the neuropsychopharmacological profile of *C. zacatechichi*, showing the likely involvement on the cholinergic and dopaminergic systems, via inhibition of AChE and tyrosinase, respectively.

3.4. *C. zacatechichi positively impacts oxidative stress by inhibiting 5-lipoxygenase (5-LOX) and scavenging free radicals*

The eicosanoid metabolizing enzyme 5-LOX is expressed in various brain regions, namely in the ventral midbrain, being involved in dopaminergic neuronal death by causing lipid peroxidation (Kang et al., 2013). Phospholipids and cholesterol, main constituents of the cell membrane and taking a core role on membrane fluidity and integrity, are main targets of the inflammatory damage that occurs through the action of 5-LOX. Worth to note that increased lipid peroxidation is also a relatively common feature of psychoactive drugs and particularly critical when occurring on the CNS, as brain tissues and cells are particularly susceptible due to their high content in polyunsaturated fatty acids (Al-Hakeim et al., 2022).

The extract obtained from the aerial parts of *C. zacatechichi* significantly inhibited the activity of 5-LOX at concentrations higher than 31.25 μg/mL ($p < 0.01$), leading to a 92.07% inhibition ($p < 0.001$) at the highest concentration tested (Fig. 4A). These results suggest not only a reduced probability of neuronal damage via lipid peroxidation but also that the aerial parts of *C. zacatechichi* exhibit anti-inflammatory effects through the inhibition of leukotriene production.

An IC_{50} value of 72.60 ± 7.3 μg/mL has been estimated, demonstrating a lower inhibitory capacity compared to quercetin (IC_{50} = 5.25 ± 1.15 μg/mL) which is used here as a reference naturally occurring inhibitor. It is plausible to infer that the strong inhibitory effect of the *C. zacatechichi* extract against 5-LOX relies on its phenolic constituents, SAR studies indicating that the preferred structural features in flavonoids include vicinal phenolic hydroxy groups at the 3′ and 4′ positions in the B ring, along with a 2,3-double bond and a 4-oxo functionality in the C ring (Ribeiro et al., 2014). Therefore, the extract's inhibitory activity may be attributed to specific flavonols, particularly to quercetin (**24**) and its derivatives **17** and **19** (Table 3), that meet such structural requirements for improved inhibitory efficiency. Moreover, specific hydroxycinnamic acid derivatives may also contribute to the observed effects, as decreases on the 5-LOX activity have been reported for caffeic acid (**5**), 5-CQA (**3**), and 3,5-diCQA (**16**).

Cumulative experimental evidence demonstrate also that an array of new psychoactive stimulants and psychedelics exert neurotoxic effects also through the enhanced production of free radicals, namely $^{\bullet}NO$ and $O_2^{\bullet-}$ (Rudin et al., 2021). Neuronal cells are also particularly vulnerable to the direct effects of reactive oxygen species (ROS) and reactive nitrogen species (RNS), due to their high lipidic content, high metabolic activity, high oxygen consumption and limited cellular regeneration capacity (Chen et al., 2022).

Rather than exacerbating the oxidative burst mediated by $^{\bullet}NO$ and $O_2^{\bullet-}$, the aqueous extract obtained from *C. zacatechichi* aerial parts was found to significantly neutralize both radicals (Fig. 4B and C). The scavenging effects were particularly evident towards $O_2^{\bullet}$, with an IC_{50} value of 56.31 ± 3.6 μg/mL being estimated, with concentrations higher than 125 μg/mL leading to a reduction in radical levels exceeding 80% (Fig. 4C). While displaying a weaker scavenging effect, *C. zacatechichi* extract caused a significant reduction in $^{\bullet}NO$ levels at concentrations ranging from 62.5 to 1000 μg/mL, with a maximum reduction of

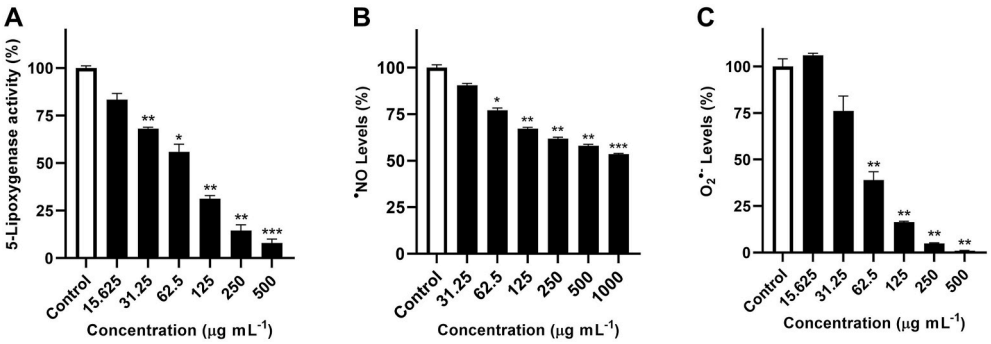

Fig. 4. Effects of *C. zacatechichi* aerial parts extract on the enzymatic activity of 5-lipoxygenase (**A**) and upon the free radicals $^{\bullet}NO$ (**B**) and $O_2^{\bullet-}$ (**C**). Results are shown as mean ± SEM from three independent experiments performed in triplicate. Statistical significance: $^{*}p < 0.05$; $^{**}p < 0.01$; $^{***}p < 0.001$.

approximately 47% at the highest concentration tested (Fig. 4B).

Considering the qualitative and quantitative chemical profiles of *C. zacatechichi* (Tables 2 and 3), the significant scavenging effects were anticipated as the most prominent bioactivity features of phenolic compounds are their antiradical and antioxidant activities, which rely on their ability to donate a hydrogen or electron and to delocalize the unpaired electron within the aromatic structure (Fernandez-Panchon et al., 2008). A major contribution from caffeic acid (**5**), the building block of the hydroxycinnamic acids, is expected as an effective scavenging agent towards both radicals (Gülçin, 2006). Specifically concerning 5-CQA (**3**), the potent radical scavenging activity towards $^{\bullet}NO$ and $O_2^{\bullet-}$ is well described, particularly through electron paramagnetic resonance (EPR) spectroscopy experiments (Watanabe et al., 2007). Regarding the flavonols identified in *C. zacatechichi* (Table 2), both quercetin and kaempferol derivatives meet the structural requirements for optimal antiradical activity, comprising the double bond at C2-C3 in conjugation with a 4-oxo function in the C-ring, which enhances the stabilization of the flavonoid phenoxyl radical (Amić et al., 2007). Furthermore, the catechol moiety in the B-ring, as seen in quercetin derivatives, confers greater stability to the resulting radicals, thereby enhancing the antiradical effects (Amić et al., 2007).

4. Conclusions

The current study delivers previously unreported data on the neuropharmacological effects and toxicity profile of "Mexican calea" (*C. zacatechichi*). The detected interference with the cholinergic system, and potentially with the dopaminergic pathway, presumably underlies the empirically claimed dream-inducing effects of the plant. Notably, strong cytotoxicity was observed in neuronal SH-SY5Y and microglial BV-2 cells, appearing to stem from apoptotic cell death at low concentrations, being independent of radical stress and lipid peroxidation. The identification of 24 previously unreported phenolic constituents enhances our understanding of the biosynthetic machinery of *C. zacatechichi* and highlights specific bioactives that contribute to its oneirogenic and antiradical effects. These findings underscore the importance of further research to fully understand the plant's safety profile and the mechanisms underlying its psychoactive effects. Ultimately, our results provide valuable insights for regulatory considerations regarding its recent use in recreational settings and contribute to resolving previous discrepancies regarding its pharmacological effects.

CRediT authorship contribution statement

Maria Rita Garcia: Writing – original draft, Investigation, Formal analysis. **Federico Ferreres:** Writing – review & editing, Methodology, Investigation, Formal analysis. **Tiago Mineiro:** Writing – original draft, Investigation, Formal analysis. **Romeu A. Videira:** Writing – review & editing, Methodology, Investigation, Formal analysis. **Ángel Gil-Izquierdo:** Writing – review & editing, Investigation, Formal analysis. **Paula B. Andrade:** Writing – review & editing, Validation, Resources, Funding acquisition. **Vítor Seabra:** Writing – review & editing, Supervision. **Diana Dias-da-Silva:** Writing – review & editing, Validation, Supervision. **Nelson G.M. Gomes:** Writing – review & editing, Validation, Supervision, Conceptualization.

Funding

This work received financial support from FCT/MCTES (UIDB/50006/2020 DOI: 10.54499/UIDB/50 006/2020) through national funds.

Declaration of competing interest

The authors declare that they have no known competing financial interests or personal relationships that could have appeared to influence the work reported in this paper.

Acknowledgments

Romeu A. Videira thanks FCT (Fundação para a Ciência e Tecnologia) for funding through CEECINST/00136/2021/CP2820/CT0001, https://doi.org/10.54499/CEECINST/00136/2021/CP2820/CT0001. Nelson G. M. Gomes thanks FCT (Fundação para a Ciência e Tecnologia) for funding through the Scientific Employment Stimulus Individual Call (Ref. 2022.07375. CEECIND); https://doi.org/10.54499/2022.07375.CEECIND/CP1724/CT0013.

Data availability

Data will be made available on request.

References

Al-Hakeim, H.K., Altufaili, M.F., Almulla, A.F., Moustafa, S.R., Maes, M., 2022. Increased lipid peroxidation and lowered antioxidant defenses predict methamphetamine induced psychosis. Cells 11. https://doi.org/10.3390/cells11223694.

Alper, K., Reith, M.E.A., Sershen, H., 2012. Ibogaine and the inhibition of acetylcholinesterase. J. Ethnopharmacol. 139, 879–882. https://doi.org/10.1016/j.jep.2011.12.006.

Amić, D., Davidović-Amić, D., Beslo, D., Rastija, V., Lucić, B., Trinajstić, N., 2007. SAR and QSAR of the antioxidant activity of flavonoids. Curr. Med. Chem. 14, 827–845. https://doi.org/10.2174/092986707780090954.

Armijos, C., Gilardoni, G., Amay, L., Lozano, A., Bracco, F., Ramirez, J., Bec, N., Larroque, C., Finzi, P.V., Vidari, G., 2016. Phytochemical and ethnomedicinal study of Huperzia species used in the traditional medicine of Saraguros in Southern Ecuador; AChE and MAO inhibitory activity. J. Ethnopharmacol. 193, 546–554. https://doi.org/10.1016/j.jep.2016.09.049.

Aru, J., Siclari, F., Phillips, W.A., Storm, J.F., 2020. Apical drive—a cellular mechanism of dreaming? Neurosci. Biobehav. Rev. 119, 440–455. https://doi.org/10.1016/j.neubiorev.2020.09.018.

Bernardo, J., Ferreres, F., Gil-Izquierdo, Á., Videira, R.A., Valentão, P., Veiga, F., Andrade, P.B., 2018. In vitro multimodal-effect of Trichilia catigua A. Juss. (Meliaceae) bark aqueous extract in CNS targets. J. Ethnopharmacol. 211, 247–255. https://doi.org/10.1016/j.jep.2017.09.039.

Bernardo, J., Santos, A.C., Videira, R.A., Valentão, P., Veiga, F., Andrade, P.B., 2022. Trichilia catigua and Turnera diffusa phyto-phospholipid nanostructures: physicochemical characterization and bioactivity in cellular models of induced neuroinflammation and neurotoxicity. Int. J. Pharm. 620, 121774. https://doi.org/10.1016/j.ijpharm.2022.121774.

Brito-da-costa, A.M., Dias-da-silva, D., Gomes, N.G.M., Dinis-oliveira, R.J., Madureira-carvalho, Á., 2020. Toxicokinetics and toxicodynamics of ayahuasca alkaloids N,N-dimethyltryptamine (DMT), harmine, harmaline and tetrahydroharmine: clinical and forensic impact. Pharmaceuticals 13. https://doi.org/10.3390/ph13110334.

Carballo-Carbajal, I., Laguna, A., Romero-Giménez, J., Cuadros, T., Bové, J., Martinez-Vicente, M., Parent, A., Gonzalez-Sepulveda, M., Peñuelas, N., Torra, A., Rodríguez-Galván, B., Ballabio, A., Hasegawa, T., Bortolozzi, A., Gelpi, E., Vila, M., 2019. Brain tyrosinase overexpression implicates age-dependent neuromelanin production in Parkinson's disease pathogenesis. Nat. Commun. 10, 973. https://doi.org/10.1038/s41467-019-08858-y.

Cebollada, P., Gomes, N.G.M., Andrade, P.B., López, V., 2024. An integrated in vitro approach on the enzymatic and antioxidant mechanisms of four commercially available essential oils (Copaifera officinalis, Gaultheria fragrantissima, Helichrysum italicum, and Syzygium aromaticum) traditionally used topically for th. Front. Pharmacol. 14. https://doi.org/10.3389/fphar.2023.1310439.

Chatatikun, M., Tedasen, A., Pattaranggoon, N.C., Palachum, W., Chuaijit, S., Mudpan, A., Pruksaphanrat, S., Sohbenalee, S., Yamasaki, K., Klangbud, W.K., 2023. Antioxidant activity, anti-tyrosinase activity, molecular docking studies, and molecular dynamic simulation of active compounds found in nipa palm vinegar. PeerJ 11, e16494. https://doi.org/10.7717/peerj.16494.

Chen, B., Zhao, J., Zhang, R., Zhang, L., Zhang, Q., Yang, H., An, J., 2022. Neuroprotective effects of natural compounds on neurotoxin-induced oxidative stress and cell apoptosis. Nutr. Neurosci. 25, 1078–1099. https://doi.org/10.1080/1028415X.2020.1840035.

Clifford, M.N., Johnston, K.L., Knight, S., Kuhnert, N., 2003. Hierarchical scheme for LC-MSn identification of chlorogenic acids. J. Agric. Food Chem. 51, 2900–2911. https://doi.org/10.1021/jf026187q.

Conforti, F., Rigano, D., Formisano, C., Bruno, M., Loizzo, M.R., Menichini, F., Senatore, F., 2010. Metabolite profile and in vitro activities of Phagnalon saxatile (L.) Cass. relevant to treatment of Alzheimer's disease. J. Enzym. Inhib. Med. Chem. 25, 97–104. https://doi.org/10.3109/14756360903018260.

Devkota, H.P., Tsushiro, K., Watanabe, T., 2022. Bioactive phenolic compounds from the flowers of Farfugium japonicum (L.) Kitam. var. giganteum (Siebold et Zucc.) Kitam. (Asteraceae). Nat. Prod. Res. 36, 4036–4039. https://doi.org/10.1080/14786419.2021.1903004.

Díaz, J.L., 1979. Ethnopharmacology and taxonomy of Mexican psychodysleptic plants. J. Psychedelic Drugs 11, 71–101. https://doi.org/10.1080/02791072.1979.10472094.
European Monitoring Centre for Drugs and Drug Addiction, 2022. European Drug Report 2022:Trends and Developments. Publications Office of the European Union.
Fernandez-Panchon, M.S., Villano, D., Troncoso, A.M., Garcia-Parrilla, M.C., 2008. Antioxidant activity of phenolic compounds: from in vitro results to in vivo evidence. Crit. Rev. Food Sci. Nutr. 48, 649–671. https://doi.org/10.1080/10408390701761845.
Ferreres, F., Grosso, C., Gil-Izquierdo, A., Fernandes, A., Valentão, P., Andrade, P.B., 2015. Comparing the phenolic profile of Pilocarpus pennatifolius Lem. by HPLC–DAD–ESI/MSn with respect to authentication and enzyme inhibition potential. Ind. Crops Prod. 77, 391–401. https://doi.org/10.1016/j.indcrop.2015.09.006.
González-Yáñez, M.G.E., Rivas-Morales, C., Oranday-Cárdenas, M.A., Verde-Star, M.J., Núñez-González, M.A., Sanchez, E., Leos-Rivas, C., 2019. Safety of aqueous extract of calea ternifolia used in Mexican traditional medicine. Evid. base Compl. Alternative Med. https://doi.org/10.1155/2019/7478152, 2019.
Gott, J.A., Stücker, S., Kanske, P., Haaker, J., Dresler, M., 2024. Acetylcholine and metacognition during sleep. Conscious. Cognit. 117, 103608. https://doi.org/10.1016/j.concog.2023.103608.
Graziano, S., Orsolini, L., Rotolo, M.C., Tittarelli, R., Schifano, F., Pichini, S., 2016. Herbal highs: review on psychoactive effects and neuropharmacology. Curr. Neuropharmacol. 15, 750–761. https://doi.org/10.2174/1570159x14666161031144427.
Greggio, E., Bergantino, E., Carter, D., Ahmad, R., Costin, G.-E., Hearing, V.J., Clarimon, J., Singleton, A., Eerola, J., Hellström, O., Tienari, P.J., Miller, D.W., Beilina, A., Bubacco, L., Cookson, M.R., 2005. Tyrosinase exacerbates dopamine toxicity but is not genetically associated with Parkinson's disease. J. Neurochem. 93, 246–256. https://doi.org/10.1111/j.1471-4159.2005.03019.x.
Gülçin, İ., 2006. Antioxidant activity of caffeic acid (3,4-dihydroxycinnamic acid). Toxicology 217, 213–220. https://doi.org/10.1016/j.tox.2005.09.011.
Herz, W., Kumar, N., 1980. Sesquiterpene lactones of Calea zacatechichi and C. urticifolia. Phytochemistry 19, 593–597. https://doi.org/10.1016/0031-9422(80)87022-1.
Jakimiuk, K., Sari, S., Milewski, R., Supuran, C.T., Şöhretoğlu, D., Tomczyk, M., 2022. Flavonoids as tyrosinase inhibitors in in silico and in vitro models: basic framework of SAR using a statistical modelling approach. J. Enzym. Inhib. Med. Chem. 37, 421–430. https://doi.org/10.1080/14756366.2021.2014832.
Jin, W., Stehbens, S.J., Barnard, R.T., Blaskovich, M.A.T., Ziora, Z.M., 2024. Dysregulation of tyrosinase activity: a potential link between skin disorders and neurodegeneration. J. Pharm. Pharmacol. 76, 13–22. https://doi.org/10.1093/jpp/rgad107.
João, K.G., Videira, R.A., Paiva-Martins, F., Valentão, P., Pereira, D.M., Andrade, P.B., 2021. Homarine alkyl ester derivatives as promising acetylcholinesterase inhibitors. ChemMedChem 16, 3315–3325. https://doi.org/10.1002/cmdc.202100265.
Josabad Alonso-Castro, A., Jose Maldonado-Miranda, J., Zarate-Martinez, A., Jacobo-Salcedo, M.D.R., Fernández-Galicia, C., Alejandro Figueroa-Zuñiga, L., Abel Rios-Reyes, N., Angel De León-Rubio, M., Andrés Medellín-Castillo, N., Reyes-Munguia, A., Méndez-Martínez, R., Carranza-Alvarez, C., 2012. Medicinal plants used in the Huasteca Potosina, México. J. Ethnopharmacol. 143, 292–298. https://doi.org/10.1016/j.jep.2012.06.035.
Kang, J.Y., Park, S.K., Guo, T.J., Ha, J.S., Lee, D.S., Kim, J.M., Lee, U., Kim, D.O., Heo, H. J., 2016. Reversal of trimethyltin-induced learning and memory deficits by 3,5-dicaffeoylquinic acid. Oxid. Med. Cell. Longev. 2016. https://doi.org/10.1155/2016/6981595.
Kang, K.-H., Liou, H.-H., Hour, M.-J., Liou, H.-C., Fu, W.-M., 2013. Protection of dopaminergic neurons by 5-lipoxygenase inhibitor. Neuropharmacology 73, 380–387. https://doi.org/10.1016/j.neuropharm.2013.06.014.
Kari, S., Subramanian, K., Altomonte, I.A., Murugesan, A., Yli-Harja, O., Kandhavelu, M., 2022. Programmed cell death detection methods: a systematic review and a categorical comparison. Apoptosis 27, 482–508. https://doi.org/10.1007/s10495-022-01735-y.
Khan, H., Marya, Amin, S., Kamal, M.A., Patel, S., 2018. Flavonoids as acetylcholinesterase inhibitors: current therapeutic standing and future prospects. Biomed. Pharmacother. 101, 860–870. https://doi.org/10.1016/j.biopha.2018.03.007.
Kim, H.H., Kim, J.K., Kim, J., Jung, S.-H., Lee, K., 2020. Characterization of caffeoylquinic acids from lepisorus thunbergianus and their melanogenesis inhibitory activity. ACS Omega 5, 30946–30955. https://doi.org/10.1021/acsomega.0c03752.
LaBerge, S., LaMarca, K., Baird, B., 2018. Pre-sleep treatment with galantamine stimulates lucid dreaming: a double-blind, placebo-controlled, crossover study. PLoS One 13, 1–16. https://doi.org/10.1371/journal.pone.0201246.
Leonti, M., Sticher, O., Heinrich, M., 2003. Antiquity of medicinal plant usage in two Macro-Mayan ethnic groups (México). J. Ethnopharmacol. 88, 119–124. https://doi.org/10.1016/S0378-8741(03)00188-0.
Li, N., Yang, J., Wang, C., Wu, L., Liu, Y., 2023. Screening bifunctional flavonoids of anti-cholinesterase and anti-glucosidase by in vitro and in silico studies: quercetin, kaempferol and myricetin. Food Biosci. 51, 102312. https://doi.org/10.1016/j.fbio.2022.102312.
Lim, D.W., Park, J., Jung, J., Kim, S.-H., Um, M.Y., Yoon, M., Kim, Y.T., Han, D., Lee, C., Lee, J., 2020. Dicaffeoylquinic acids alleviate memory loss via reduction of oxidative stress in stress-hormone-induced depressive mice. Pharmacol. Res. 161, 105252. https://doi.org/10.1016/j.phrs.2020.105252.
Martinez-Mota, L., Cruz-Tavera, A., Dorantes-Barrón, A.M., Arrieta-Báez, D., Ramírez-Salado, I., Cruz-Aguilar, M.A., Mayagoitia-Novales, L., Cassani, J., Estrada-Reyes, R., 2021. Calea zacatechichi Schltdl. (Compositae) produces anxiolytic- and antidepressant-like effects, and increases the hippocampal activity during REM sleep in rodents. J. Ethnopharmacol. 265. https://doi.org/10.1016/j.jep.2020.113316.
Martinez, M., Esquivel, B., Ortega, A., 1987. Two caleines from Calea zacatechichi. Phytochemistry 26, 2104–2106. https://doi.org/10.1016/S0031-9422(00)81769-0.
Mata, R., Contreras-Rosales, A.J., Gutiérrez-González, J.A., Villaseñor, J.L., Pérez-Vásquez, A., 2022. Calea ternifolia Kunth, the Mexican "dream herb". a concise review. Botany 100, 261–274. https://doi.org/10.1139/cjb-2021-0063.
Mayagoitia, L., Díaz, J.L., Contreras, C.M., 1986. Psychopharmacologic analysis of an alleged oneirogenic plant: calea zacatechichi. J. Ethnopharmacol. 18, 229–243. https://doi.org/10.1016/0378-8741(86)90002-4.
Mossoba, M.E., Flynn, T.J., Vohra, S., Wiesenfeld, P., Sprando, R.L., 2016. Evaluation of "dream herb," calea zacatechichi, for nephrotoxicity using human kidney proximal tubule cells. J. Toxicol. 2016. https://doi.org/10.1155/2016/9794570.
Oldoni, A.A., Bacchi, A.D., Mendes, F.R., Tiba, P.A., Mota-Rolim, S., 2024. Neuropsychopharmacological induction of (lucid) dreams: a narrative review. Brain Sci. https://doi.org/10.3390/brainsci14050426.
Pagel, J.F., Helfter, P., 2003. Drug induced nightmares - an etiology based review. Hum. Psychopharmacol. 18, 59–67. https://doi.org/10.1002/hup.465.
Quijano, L., Romo de Vivar, A., Rios, T., 1979. Revision of the structures of caleine A and B, germacranolide sesquiterpenes from Calea zacatechichi. Phytochemistry 18, 1745–1747. https://doi.org/10.1016/0031-9422(79)80203-4.
Reissner, K.J., Kalivas, P.W., 2010. Using glutamate homeostasis as a target for treating addictive disorders. Behav. Pharmacol. 21, 514–522. https://doi.org/10.1097/FBP.0b013e32833d41b2.
Ribeiro, D., Freitas, M., Tomé, S.M., Silva, A.M.S., Porto, G., Cabrita, E.J., Marques, M.M. B., Fernandes, E., 2014. Inhibition of LOX by flavonoids: a structure-activity relationship study. Eur. J. Med. Chem. 72, 137–145. https://doi.org/10.1016/j.ejmech.2013.11.030.
Ribeiro, V., Ferreres, F., Macedo, T., Gil-Izquierdo, Á., Oliveira, A.P., Gomes, N.G.M., Araújo, L., Pereira, D.M., Andrade, P.B., Valentão, P., 2021. Activation of caspase-3 in gastric adenocarcinoma AGS cells by Xylopia aethiopica (Dunal) A. Rich. fruit and characterization of its phenolic fingerprint by HPLC-DAD-ESI(Ion Trap)-MS(n) and UPLC-ESI-QTOF-MS(2). Food Res. Int. 141, 110121. https://doi.org/10.1016/j.foodres.2021.110121.
Rudin, D., Liechti, M.E., Luethi, D., 2021. Molecular and clinical aspects of potential neurotoxicity induced by new psychoactive stimulants and psychedelics. Exp. Neurol. 343, 113778. https://doi.org/10.1016/j.expneurol.2021.113778.
Sachet, M., Liang, Y.Y., Oehler, R., 2017. The immune response to secondary necrotic cells. Apoptosis 22, 1189–1204. https://doi.org/10.1007/s10495-017-1413-z.
Sałaga, M., Fichna, J., Socała, K., Nieoczym, D., Pieróg, M., Zielińska, M., Kowalczuk, A., Wlaź, P., 2016. Neuropharmacological characterization of the oneirogenic Mexican plant Calea zacatechichi aqueous extract in mice. Metab. Brain Dis. 31, 631–641. https://doi.org/10.1007/s11011-016-9794-1.
Santi, M.D., Bouzidi, C., Gorod, N.S., Puiatti, M., Michel, S., Grougnet, R., Ortega, M.G., 2019. In vitro biological evaluation and molecular docking studies of natural and semisynthetic flavones from Gardenia oudiepe (Rubiaceae) as tyrosinase inhibitors. Bioorg. Chem. 82, 241–245. https://doi.org/10.1016/j.bioorg.2018.10.034.
Shoukat, S., Zia, M.A., Uzair, M., Attia, K.A., Abushady, A.M., Fiaz, S., Ali, S., Yang, S.H., Ali, G.M., 2023. Bacopa monnieri: a promising herbal approach for neurodegenerative disease treatment supported by in silico and in vitro research. Heliyon 9, e21161. https://doi.org/10.1016/j.heliyon.2023.e21161.
Si, Y.-X., Yin, S.-J., Oh, S., Wang, Z.-J., Ye, S., Yan, L., Yang, J.-M., Park, Y.-D., Lee, J., Qian, G.-Y., 2012. An integrated study of tyrosinase inhibition by rutin: progress using a computational simulation. J. Biomol. Struct. Dyn. 29, 999–1012. https://doi.org/10.1080/073911012010525028.
United Nations Office on Drugs and Crime, 2013. The Challenge of New Psychoactive Substances.
Venegas-Flores, H., Segura-Cobos, D., Vázquez-Cruz, B., 2002. Antiinflammatory activity of the aqueous extract of Calea zacatechichi. Proc. West. Pharmacol. Soc. 45, 110–111.
Verzella, D., Pescatore, A., Capece, D., Vecchiotti, D., Ursini, M.V., Franzoso, G., Alesse, E., Zazzeroni, F., 2020. Life, death, and autophagy in cancer: NF-κB turns up everywhere. Cell Death Dis. 11, 210. https://doi.org/10.1038/s41419-020-2399-y.
Viany, L., Rizal, R., Widowati, W., Samin, B., Kusuma, R., Fachrial, E., Nyoman, L.E.I., 2019. Comparison of antioxidant and antiaging activities between dragon fruit (Hyloceureus polyrhizus (F.A.C. Weber) Britton & Rose) rind extract and kaempferol. Maj. Kedokt. Bandung 51, 147–153. https://doi.org/10.15395/mkb.v51n3.1715.
Wang, Yunliang, Wang, Yutong, Li, J., Hua, L., Han, B., Zhang, Y., Yang, X., Zeng, Z., Bai, H., Yin, H., Lou, J., 2016. Effects of caffeic acid on learning deficits in a model of Alzheimer's disease. Int. J. Mol. Med. 38, 869–875. https://doi.org/10.3892/ijmm.2016.2683.
Watanabe, S., Hashimoto, K., Tazaki, H., Iwamoto, Y., Shinohara, N., Satoh, K., Sakagami, H., 2007. Radical scavenging activity and inhibition of macrophage NO production by fukinolic acid, a main phenolic constituent in Japanese butterbur (Petasites japonicus). Food Sci. Technol. Res. 13, 366–371. https://doi.org/10.3136/fstr.13.366.
Wu, H., Fronczek, F., Burandt, C., Zjawiony, J., 2011. Antileishmanial germacranolides from calea zacatechichi. Planta Med. 77, 749–753. https://doi.org/10.1055/s-0030-1250584.
Zhao, J., Zhang, W., Wu, T., Wang, H., Mao, J., Liu, J., Zhou, Z., Lin, X., Yan, H., Wang, Q., 2021. Efferocytosis in the central nervous system. Front. Cell Dev. Biol. 9. https://doi.org/10.3389/fcell.2021.773344.